MODEL-BASED UXO CLASSIFICATION BASED ON STATIC 3-COMPONENT TEM MEASUREMENTS

Scott C. MacInnes, Donald D. Snyder, David C. George, and Kenneth L. Zonge
Zonge Engineering & Research Organization, Tucson, AZ

Abstract

The dipole model characterized by an anisotropic polarizability tensor is well accepted as a valid model describing the EM behavior of electrically small, highly conductive metal objects such as UXO. The model has been used successfully to characterize and classify EM anomalies acquired with single-gate TEM metal detectors such as the EM-61. Successful inversion of EM-61 anomalies using this dipole model depends on measurements at many points within a small radius of the target. Since these measurements are acquired dynamically, survey specifications in terms of line-spacing and survey speed must be tight in order to be assured of acquiring a sufficient number of independent data to robustly parameterize the target for classification.

An alternate method of characterizing an anomaly is to reacquire it and to take more precise data by locating the antenna array at a few discrete stations in a pattern referenced to the center of the observed anomaly. In this paper, we describe experiments in UXO characterization using a multi-gate 3-component fast TEM (NanoTEM®) system. With this system, three orthogonal receiver antennas simultaneously acquire 31-gate TEM transients. The 3-component data triple the number of independent data measurements supplied at each field point. Using this system, we have acquired data sets using two methodologies. In the first methodology, we take measurements with a 3-component cart system at 5 locations centered on the anomaly peak, thus acquiring 15 31-gate transients for use in the dipole inversion. In the second methodology, we use an array of flat-lying loops arranged to illuminate in 3 orthogonal directions and measure the target's polarization response over a range of angles. Both data sets assure that the UXO has been polarized in its 3 principal directions. The dipole model simultaneously models both time and spatial components of the measured fields and reports a three-dimensional target position, spatial attitude, and polarizability parameters (i.e., the "beta" parameters) as a function of time. Results from characterization of various UXO and non-UXO targets models buried locally in Tucson and from the NRL Baseline Ordnance Classification Test site at Blossom Pt will be used to illustrate the technique.

Introduction

Multipurpose geophysical receivers can be reconfigured to suit survey needs. When mapping a grid area to locate UXO it is common to use a cart mounted TEM system with a horizontal transmitter loop and three more receiver loops arranged to measure multiple magnetic field components (Figure 1). Small transmitter and receiver loops are optimal for detecting near-surface conductors. With a different loop arrangement, the same TEM equipment was used to map conductors on the bottom of a frozen lake. Figure 2 shows a sled-mounted NanoTEM system with 4.6 by 4.6 m transmitter and 1.5 by 1.5 m receiver loops. The larger loops improved the response from deeper targets, in this case metallic objects on the bottom of a 6 m deep lake.

Figure 1: A cart-mounted Dynamic NanoTEM (DNT) system configured with a 1 by 1 m horizontal transmitter loop and three 0.5 by 0.5 m receiver loops arranged to measure x, y and z-component secondary magnetic fields. The smaller loops are optimal for detecting shallow objects at depths of 2 m or less.

Figure 2: A sled mounted NanoTEM system configured with a 4.6 by 4.6 m transmitter loop and a single 1.5 by 1.5 m horizontal receiver loop for locating UXO on the bottom of a frozen lake. Larger loops were used to improve the response from conductive objects on the bottom of the 6 m deep lake.

Electromagnetic source fields are generated by driving square current pulses of alternating polarity separated by zero current measurement intervals through the transmitter loop (Figure 3). During the intervals between current pulses, currents induced in conductive metallic objects are detected by measuring dB/dt transients with the receiver loops. DNT transient values are saved at 31 time windows spaced logarithmically between 0.1 and 2000 µsec after each current pulse (Figure 4).

dB/dt transient shapes record diagnostic information about UXO properties. Induced currents decay more slowly in larger or more conductive objects. Elongated objects have an anisotropic response with a more persistent signal along the long axis than along shorter transverse axes. Transient characteristics are also affected by UXO properties like object shape and permeability.
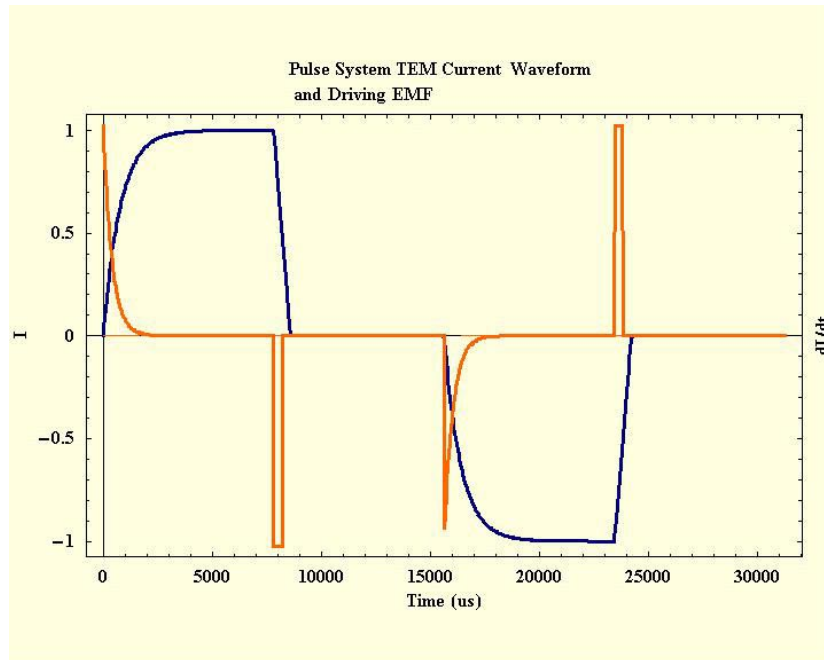
Figure 3: Transmitter current and receiver dB/dt waveforms for a pulse TEM system. Current pulses of alternating polarity are driven through the transmitter loop (blue curve). As the transmitter current is driven to zero at the end of each current pulse, the collapsing magnetic source field generates a large dB/dt pulse in the receiver loops (orange curve). The weak secondary dB/dt responses generated by currents induced in subsurface metallic objects can be measured while the transmitter current is off.
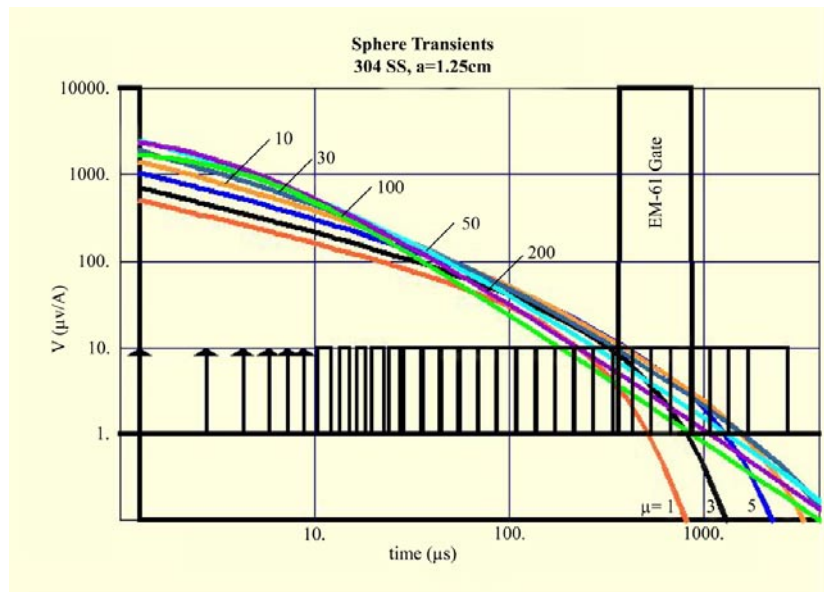

Figure 4: Receiver loop dB/dt transients versus log time. The NanoTEM system records transient values at 31 time windows spaced logarithmically between 0.1 and 2000 μsec after the transmitter current pulse. Transient shape can provide diagnostic information about UXO properties. Colored curves show the different transient responses expected from a conductive spherical object with relative permeability values ranging from 1 to 200.

3

Dipole Model

An anisotropic dipole model is suitable for predicting the response of compact, conductive objects in a resistive background. Inductive coupling between transmitter loop and target is represented by $\overline{H}_{Tx}(\overline{r}')$, the free-space magnetic field at the target generated by a unit current in the transmitter loop. As the transmitter current pulse is shut off it illuminates the target with a dB/dt spike, inducing a dipolar polarization, $\overline{M}(t,\overline{r}') = \overline{\overline{P}}(t) \cdot \overline{H}_{Tx}(\overline{r}') \cdot \delta(t)$. The target's polarization, $\overline{M}(t,\overline{r}')$, typically has a different orientation than the transmitter's magnetic field due to the target's elongation and tilt. Inductive coupling between the polarized target and a receiver loop is represented by $\overline{H}_{Rx}(\overline{r})$.
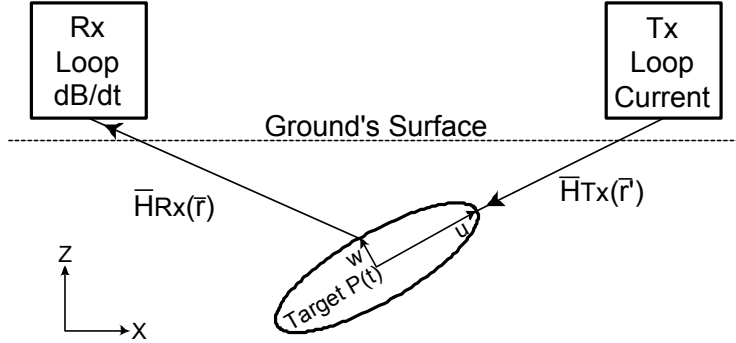

Figure 5: Schematic of an anisotropic dipole model. An elongated target will have stronger polarization along its longitudinal u axis than along its transverse v and w axes

The inductive link from transmitter loop current to target polarization and back to a receiver loop dB/dt can be represented by

$$\frac{dB(\overline{r},t,\overline{r}')}{dt} = \mu_0 \cdot \overline{H}_{Rx}(\overline{r}) \cdot \overline{\overline{P}(t)} \cdot \overline{H}_{Tx}(\overline{r}') \cdot \delta(t)$$

$\overline{H}_{Tx}(\overline{r}')$ and $\overline{H}_{Rx}(\overline{r})$ are dependent upon the locations of transmitter and receiver loops relative to the target. The model's dependence upon target (x,y,z) is contained in $\overline{H}_{Tx}(\overline{r}')$ and $\overline{H}_{Rx}(\overline{r})$ which each have units of $1/m^3$. All of the target's time-dependant behavior is described by the tensor polarizability, $\overline{\overline{P}(t)}$. For TEM modeling, convenient units for $\overline{\overline{P}(t)}$ are $cm^3/\mu sec = m^3/sec$.

$$\overline{\overline{P}(t)} = \begin{bmatrix} p_{xx}(t) & p_{xy}(t) & p_{xz}(t) \\ p_{yx}(t) & p_{yy}(t) & p_{yz}(t) \\ p_{zx}(t) & p_{zy}(t) & p_{zz}(t) \end{bmatrix} = \overline{\overline{R(\theta,\phi,\varphi)}}^t \cdot \begin{bmatrix} p_u(t) & 0 & 0 \\ 0 & p_v(t) & 0 \\ 0 & 0 & p_w(t) \end{bmatrix} \cdot \overline{\overline{R(\theta,\phi,\varphi)}}$$

$\overline{\overline{P(t)}}$ is a symmetric tensor which can be diagonalized by a rotation from geographic (x,y,z) to target axis (u,v,w) coordinates. An unrotated polarizability tensor can be parameterized by six parameters (p_{xx}, $p_{yx} = p_{xy}$, p_{yy}, $p_{zx} = p_{xz}$, $p_{zy} = p_{yz}$, p_{zz}). When rotated, polarizability is a function of ($\theta,\phi,\varphi,p_u,p_v,p_w$) where θ,ϕ, and φ are Euler rotation angles and p_u,p_v, and p_w are polarizability values along target axes.

TEM dB/dt transient data can be inverted to recover target properties by rearranging the dipole model to express dB/dt as a function of target (x,y,z) and polarizability, $\overline{\overline{P(t)}}$. Since all of the target's

time-dependant properties are contained in $\overline{\overline{P(t)}}$, an inversion to recover target position and orientation can be separated from inversion to recover a description of target polarizability time variance.

For inversion to recover target position and orientation, each TEM transient can be collapsed to a single scalar value by using a weighted sum,

$$dobs_j = \sum_i \frac{dB(t_i, r_j)}{dt} \cdot wt_i \cdot wr_j$$

$$where \quad wt_i = 1 \bigg/ \sqrt{\left(\varepsilon r_j^2 + \frac{dB(t_i, r_j)}{dt} \right)}$$

$$and \quad wr_j = 1/\varepsilon r_j = 1/transient\ noise\ levels$$

Data for each transient delay time is weighted by wt_i, a measure of signal strength for time t_i, so that so that early-time values with amplitudes near 10^5 $\mu V/Am^2$ do not completely dominate late time data with amplitudes below 1 $\mu V/Am^2$. wr_j weighting accounts for any background level differences between transients.

As Bell, et al (2001) point out, given a target (x,y,z) location, inverting $\overline{d_{obs}}$ to find the elements of an unrotated polarizability tensor is a linear least squares problem. A global inversion method like simulated annealing can be used to select trial values of the non-linear parameters target (x,y,z). For each trial (x,y,z), linear least-squares can be used to solve for p in the linear system:

$$\overline{d_{obs}} = \overline{\overline{A}} \cdot \begin{bmatrix} p_{xx} \\ p_{xy} = p_{yx} \\ p_{yy} \\ p_{zx} = p_{xz} \\ p_{zy} = p_{yz} \\ p_{zz} \end{bmatrix}$$

Individual terms of the sensitivity matrix, $\overline{\overline{A}}$, are non-linear functions of target (x,y,z). Fortunately the location of the target anomaly peak is a good estimate of target (x,y) and anomaly width is a good estimate of target depth, z, so a nonlinear inversion for target (x,y,z) can be initialized with a good starting model.

Once a satisfactory target location (x,y,z) is established, a singular value decomposition of $\overline{\overline{P(t)}}$ yields the coordinate rotation necessary to diagonalize the polarizability tensor. With a target rotation and orientation in hand, the dipole model can be used to project $\frac{dB(t_i, r_j)}{dt}$ onto the target axes. The projection generates a set of observed polarizability data $(p_u(t_i), p_v(t_i), p_w(t_i))$ which compactly describes the target's time dependent behavior. Polarizability for each axis can be parameterized by numerically integrating $p_*(t_i)$ (in $cm^3/usec$) to get a $p0_*$ (in cm^3) or by using a model like Pasion and Oldenburg's (1999):

$$p(t) = k \cdot \exp(-t/\tau) \cdot (a+t)^{-b}$$

Survey Configurations

When traversing a grid area to map UXO, measurements are taken along closely spaced lines, typically separated by one transmitter loop width or less. Saving stacked and averaged transients every 0.25 seconds produces data values every 0.25 m along line at a typical walking speed of 1 m/sec. The sampling interval along line is generally smaller than the line separation (Figure 6a).

Improved information about UXO properties can be deduced by collecting additional follow-up data. In follow up, static measurements with longer stacking times can reduce dB/dt transient noise levels by a factor of 10 or more. Additionally, loop position and orientation relative to a central survey point can be carefully measured, effectively removing the equipment location uncertainties that degrade data collected with a moving TEM system (Barrow and Nelson, 2001). Finally, since the TEM system doesn't have to be cart-mounted, a wide range of survey configurations are possible. Two possible follow up survey configurations are shown in Figures 6b and 6c.

Plan Map of TEM Survey Configurations

(a) Line data with 3-component cart

(b) 5-spot follow up 3-component cart
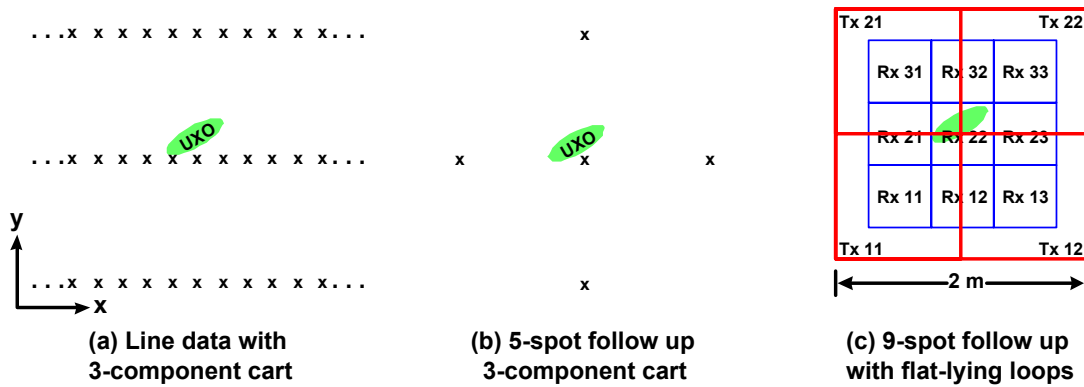
(c) 9-spot follow up with flat-lying loops

Figure 6: Plan map of TEM survey configurations. (a) Cart mounted systems generally produce data sets with a higher sampling density along line than across line. As the line may pass to one side of a target object, the y-component is particularly helpful in estimating the target's lateral position (y coordinate). (b) 3-component cart-mounted equipment can be used in a 5-spot array over the target anomaly. (c) A fixed-loop survey configuration with transmitter and receiver loops lying on the ground maximizes signal strength, allows transmitter field illumination of the target in three orthogonal directions, and interrogates the target's polarization over a range of orientations.

Figure 6b shows measurement positions for a 5-spot array using a 3-component cart-mounted system. Although the 3-component 5-spot has fewer sample points than 3-component line data, extended stacking with stationary loops reduces background noise levels so much that target model parameter estimates are improved.

Figure 6c shows a 9-spot array using flat-lying transmitter and receiver loops. Putting loops on the ground maximizes signal strength. Source field orientation is achieved by using the four transmitter loops in three different combinations. Targets can be illuminated with a horizontal source field by using a flat-lying figure-8 loop, as shown schematically in Figures 7a and 7b. Vertical source fields can be generated with a large horizontal loop as shown in Figure 7c. By using each transmitter loop configuration in turn, the target is illuminated with magnetic fields oriented in three orthogonal directions.

With each different target illumination orientation, the target response can be interrogated by making measurements at each of the receiver loops shown in Figures 6 and 7. With a three-channel receiver, it only takes three measurement sets to record transients for all nine receiver loops. By using a 3-axis receiver loop array from the DNT cart, an additional 3-component measurement can be made at the center of the follow-up array to get information about vertical field gradients and improve estimates of target depth.

The orientations of both target transmitter illumination and receiver interrogation fields should vary enough to resolve target polarizability on all three axes. Field strengths should also be as strong as possible to maximize signal to noise ratios.

Fixed-Loop TEM Tx Scanning Sequence

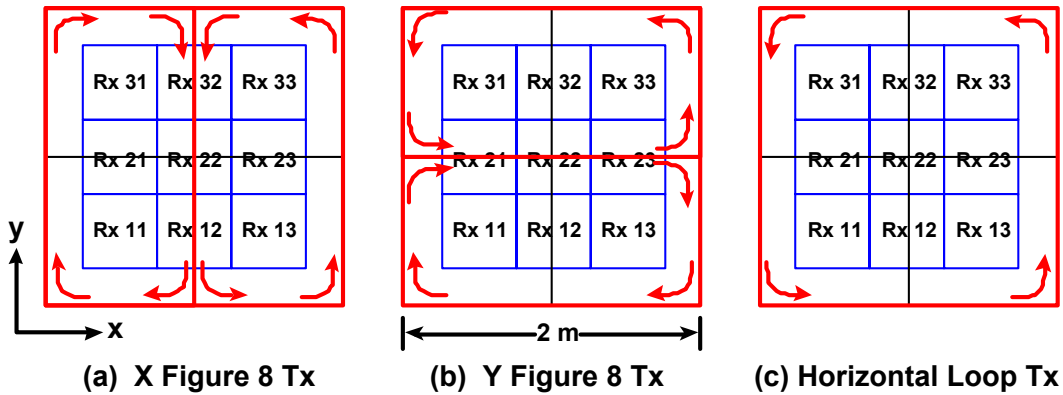(a) X Figure 8 Tx (b) Y Figure 8 Tx (c) Horizontal Loop Tx

Figure 7: Fixed-Loop TEM transmitter scanning sequence. (a) A x-directed figure-8 Tx loop illuminates a target under the loop with a magnetic field parallel to the x axis. (b) A y-directed figure-8 Tx loop illuminates target with a magnetic field parallel to the y axis. (c) A horizontal transmitter loop illuminates target with a vertical magnetic field.
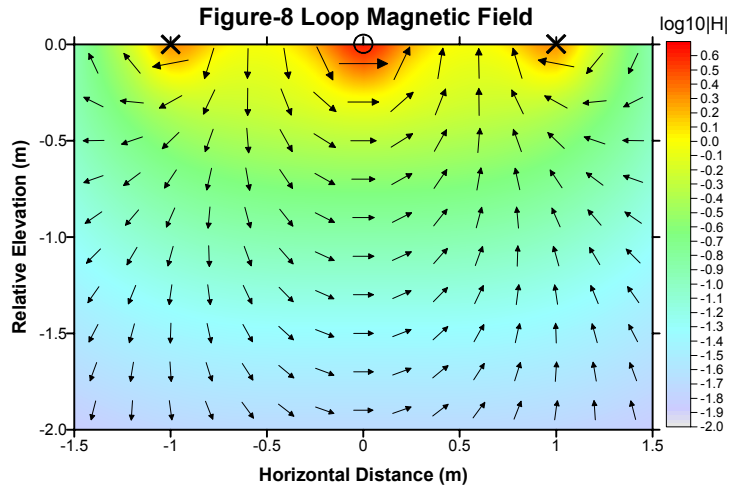

Figure 8: Cross section of figure-8 loop magnetic field direction and amplitude. A figure-8 loop produces a horizontal magnetic field in the region directly under the center of the loop. Near the center of the loop, currents in the two central wire segments produce a strong magnetic field with the cylindrical pattern and $1/r$ fall off characteristic of magnetic fields near a straight current filament. At distances much greater than one loop diameter, figure-8 loop magnetic field amplitude falls off in proportion to $1/r^4$.
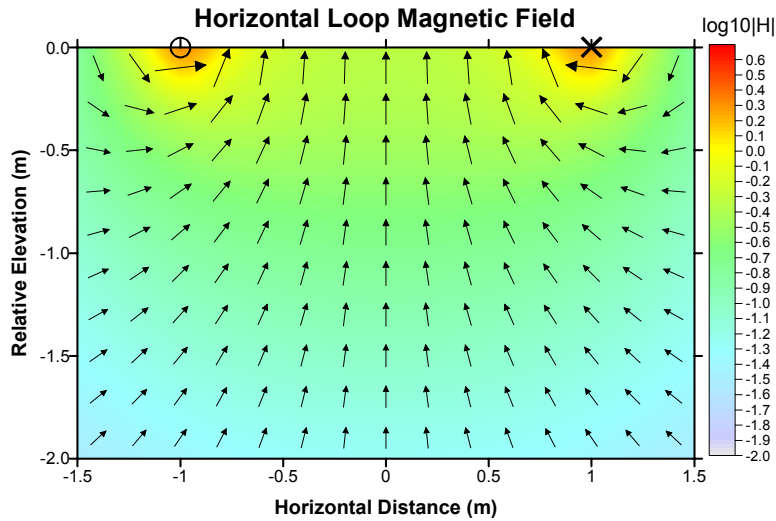
Figure 9: Cross section of horizontal loop magnetic field direction and amplitude. A horizontal loop produces a vertical magnetic field across a broad region under the center of the loop. At distances much greater than one loop diameter, horizontal loop magnetic field amplitude falls off in proportion to $1/r^3$.
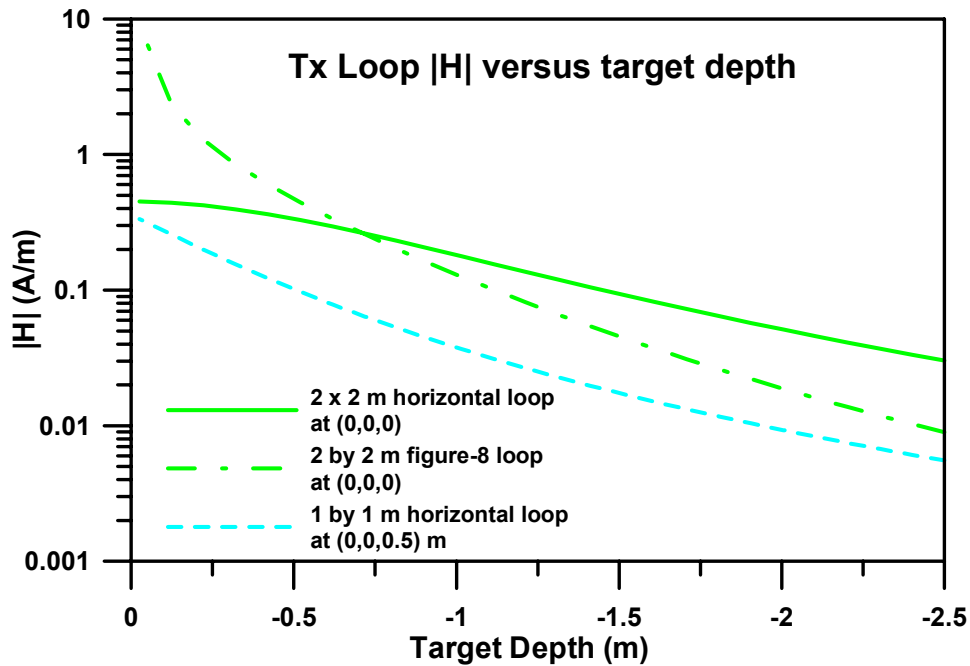

Figure 10: Transmitter loop magnetic field strength versus target depth. At the ground's surface, a 2 by 2 m horizontal loop lying on the ground's surface (solid green line) has the same field strength as a 1 by 1 m, cart-mounted loop 0.5 m above the ground (dashed blue). With increasing depth, magnetic field strengths below the center of the 1 by 1 m cart-mounted loop drop off more rapidly than for the 2 by 2 m horizontal fixed loop. Placing loops on the ground (green lines) increases signal strength relative to cart-mounted equipment (blue line).
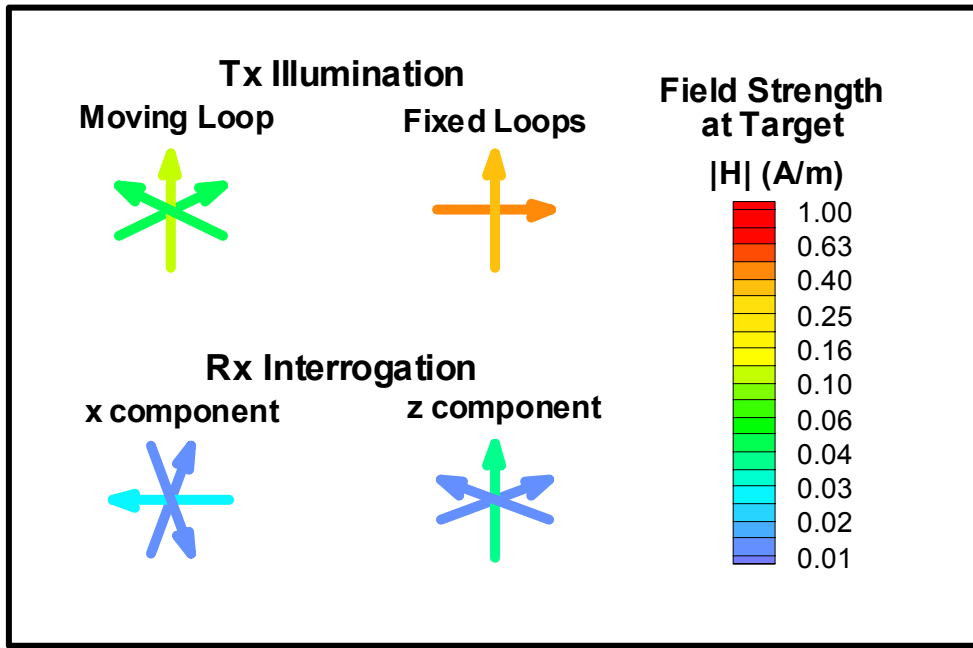
8

Tx Illumination

Moving Loop **Fixed Loops**

Field Strength at Target

|H| (A/m)

1.00
0.63
0.40
0.25
0.16
0.10
0.06
0.04
0.03
0.02
0.01

Rx Interrogation

x component **z component**

Figure 11: Target illumination by the transmitter's magnetic field and interrogation of the target's response by the receiver field. Both cart-mounted moving-loop and fixed-loop transmitters excite all axes of a target at a depth of 0.5 m. Fixed-loop transmitters generate larger field strengths at the target, since they are placed right on the ground's surface. Moving either x or z component receiver loops from side to side above the target interrogates all axes of the target's response to illumination. Signal strength is maximized when the loops are directly above the target and as close to the ground as possible.

Predicted model-parameter error

Parameter	Line XYZ	5 spot XYZ	9 spot Z	Units
dB/dt error	1	0.1	0.1	μV/A
pxx	1682.4	335.8	11.4	cm^3/μsec
pyx = pxy	408.5	117.4	4.9	cm^3/μsec
pyy	1441.9	319.7	10.8	cm^3/μsec
pzx=pxz	848.7	164.7	3.2	cm^3/μsec
pzy=pyz	915.3	204.4	5.1	cm^3/μsec
pzz	3751.9	849.6	16.5	cm^3/μsec
x	0.368	0.075	0.003	m
y	0.391	0.091	0.002	m
z	0.693	0.157	0.003	m

Table 1: Predicted model-parameter error for the three survey configurations shown in figure 7. Errors are for a spherical target at (0.1,0.2,-0.5) with a polarizability of 10^3 cm^3/usec. Transient dB/dt error levels are adjusted to reflect the difference between a dynamic 3-component cart survey (Line XYZ), and static measurements with a 3-component cart (5 spot XYZ) or a fixed-loop survey (9 spot Z).

Percent model-parameter error relative to cart XYZ line data

Parameter	Line XYZ	5 spot XYZ	9 spot Z	Units
dB/dt error	1	0.1	0.1	μV/A
pxx	100	20.0	0.7	%
pyx = pxy	100	28.7	1.2	%
pyy	100	22.2	0.7	%
pzx=pxz	100	19.4	0.4	%
pzy=pyz	100	22.3	0.6	%
pzz	100	22.6	0.4	%
x	100	20.3	0.8	%
y	100	23.2	0.6	%
z	100	22.6	0.5	%
Average %	100	22.4	0.6	%

Table 2: Predicted model-parameter error shown as a percentage relative to a dynamic 3-component cart survey. Although a static 5-spot has fewer sample points than line data, it has lower model parameter error because increased stacking time lowers dB/dt transient error levels by a factor of 10 or more. The fixed-loop 9-spot data set is improved both because of increased stacking time and because of greater signal strength from loops place right on the ground's surface.

Summary

With versatile, broadband TEM equipment it is possible to gather information that describes UXO location, orientation and time-dependent polarizability properties. Data from mapping surveys using cart-mounted equipment are degraded by motion during measurement and by uncertainties in cart position and orientation. Follow-up surveys using static measurements provide complimentary data to improve estimates of UXO model parameters. Stacking times can be increased during static measurements, significantly reducing noise levels. Loop position and orientation relative to a local control point can be carefully controlled, removing uncertainty about equipment position.

Since the equipment used for follow-up measurement does not have to be cart mounted, a wide range of loop arrangements is possible. Putting loops on the ground minimizes loop-to-target separation and maximizes signal strengths. A combination of figure-8 and horizontal transmitter-loops can be used to illuminate the target in mutually orthogonal directions. In combination with the fixed-loop transmitter array, an array of nine flat-lying receiver loops provides maximum signal strength while interrogating target polarization over a sufficient range of orientations.

It is advantageous to combine data from cart-mounted loops, elevated above the ground, with data from flat-lying loops, so that the inversion has information about both horizontal and vertical magnetic field gradients. Just as measurements at different (x,y) offsets generate information about horizontal field gradients, measurements at more than one elevation produce information about vertical gradients. Adding vertical gradient information reduces error in target depth estimates and consequently improves estimates of target polarizability.

References

1. Barrow, B. and Nelson, H.H., 2001, Model-based characterization of electromagnetic induction signatures obtained with the MTADS electromagnetic array, IEEE Tran. on Geos. and Remote Sensing, v6, pp1279-1285.
2. Bell, T.H., Barrow, J., Miller, J.T., 2001, Subsurface discrimination using electromagnetic induction sensors, IEEE Tran. on Geos. and Remote Sensing, v6, pp1286-1293.
3. Pasion, L.R., Oldenburg, D.W., 1999, Locating and determining dimensionality of UXOs using time domain induction, in SAGEEP 1999, Oakland, CA.